

[1] J.P. Morniroli, J.W. Steeds, *Ultramicroscopy* **1992**, 45, 219-239. [2] R. Vincent, P.A. Midgley, *Ultramicroscopy* **1994**, 53, 271-282. [3] M. Tanaka, M. Terauchi, *JEOL LTD*, **1985**, 156-159.

**Keywords:** microdiffraction, precession, multibeam

### MS33.P02

*Acta Cryst.* (2011) **A67**, C441

#### The study of wide-angle incidence X-Ray nano-wires using crystal asymmetric surface diffraction

Hsin-Yi Chen,<sup>a</sup> Chia-Cheng Lin,<sup>a</sup> Yung-Shih Fang,<sup>a</sup> Yi-Wei Tsai,<sup>a</sup> Chia-Hung Chu,<sup>a</sup> and Shih-Lin Chang,<sup>a,b</sup> <sup>a</sup>*Department of Physics, National Tsing Hua University, Hsinchu, (Taiwan)*. <sup>b</sup>*National Synchrotron Radiation Research Center, Hsinchu, (Taiwan)*. E-mail: hychen@ms93.url.com.tw

Wide-angle incident x-ray Si-wires are devised by using crystal asymmetric surface diffraction. The Si (113) is chosen as an asymmetric surface diffraction for the photon energy 8.8785 keV according to the Si crystal orientation and diffraction geometry. The asymmetric surface diffracted beam propagates along [110] if the incident beam is parallel to [110].  $2\theta$ -scan (vertical) shows two diffraction peaks; one is the Si(113) Bragg diffraction, and the other is its surface specular reflection. The position of the specular reflection does not vary with photon energy in the range from  $E=9.05$  keV to  $E=8.75$  keV. The positions of these two peaks in vertical ( $2\theta$ -scan) and horizontal (beta-scan) direction also depend on azimuth angle around [001], which is the angle between [110] and the incident-beam direction. The behavior of the diffracted beams in the vertical direction is governed by the photon energy and azimuth angle. In addition, interference patterns of specular reflection in the vertical direction are detected. The oscillatory intensity is related to the azimuth angle and extinction length, which we believe is a dynamical diffraction effect. The experimental results are in good agreement with the theoretical calculations using the dynamical theory of x-ray diffraction. In conclusion, we have studied the wide-angle incidence x-ray Si-wires using crystal asymmetric surface diffraction. This idea can be applied to design a new type wide-angle incidence x-ray optics using crystal surface diffraction.

**Keywords:** asymmetric-surface-diffraction

### MS33.P03

*Acta Cryst.* (2011) **A67**, C441

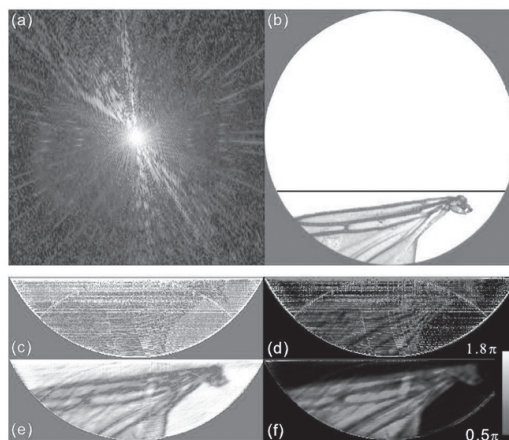
#### Implementation of a direct approach to coherent diffractive imaging

Andrew J. Morgan,<sup>a</sup> Adrian J. D'Alfonso,<sup>a</sup> Andrew V. Martin,<sup>b</sup> Alexis I. Bishop,<sup>c</sup> Leslie J. Allen,<sup>a</sup> <sup>a</sup>*School of Physics, University of Melbourne, Victoria, (Australia)*. <sup>b</sup>*Center for Free-Electron Laser Science, DESY, Hamburg (Germany)*. <sup>c</sup>*School of Physics, Monash University, Victoria (Australia)*. E-mail: andyofmelbourne@gmail.com

We present a strategy to obtain a high-fidelity reconstruction of the exit-surface wave of an object from its diffraction pattern. The direct solution of a set of linear equations extracted from the inverse Fourier transform of the diffraction pattern (which is the autocorrelation of the exit-surface wave) [1,2] is followed by a simple regularization step in which the solution is also made consistent with the non-linear information in the autocorrelation. This approach is illustrated using the diffraction pattern of a gnat's wing, illuminated with a laser. By considering residuals and condition numbers the well-posedness

(uniqueness and consistency) of the reconstruction can be analyzed.

The figure below shows the results as follows: (a) The far-field diffraction pattern of a gnat's wing illuminated with a HeNe laser. (b) A magnified image of the gnat's wing. The black horizontal line indicates the area assumed to contain the object in the linear retrieval method. In (c) we have the retrieved intensity and in (d) the change in phase of the incident wave due to the wing after the solution of the linear equations and prior to the regularization step. After the regularization step we obtain the image shown in (e) and the phase in (f). In the figure the brightness of the phase images have been scaled by the wave's intensity.



[1] A.V. Martin, L.J. Allen, *Optics Communications*, **2008**, 281, 5114-5121 [2] A.V. Martin, A.I. Bishop, D.M. Paganin, L.J. Allen, *Ultramicroscopy*, **2011**, in press, doi:10.1016/j.ultramic.2010.10.003.

**Keywords:** coherence, diffraction, imaging

### MS33.P04

*Acta Cryst.* (2011) **A67**, C441-C442

#### Observation of topography using resonant scattering and its SEM images

Riichirou Negishi,<sup>a</sup> Tomoe Fukamachi,<sup>a</sup> Kenji Hirano,<sup>a</sup> Yoshinobu Kanematsu,<sup>a</sup> Keiichi Hirano,<sup>b</sup> Takaaki Kawamura,<sup>c</sup> <sup>a</sup>*Saitama Institute of Technology*, <sup>b</sup>*KEK-PF*, <sup>c</sup>*University of Yamanashi (Japan)*. E-mail: negishi@sit.ac.jp

Near the K-absorption edge of a constituent atom in a crystal, X-ray rocking curves from the crystal sometimes show significant change with small change of X-ray energy due to resonant scattering.

Fig.1 shows measured GaAs 200 diffracted rocking curves  $I_h$ , and transmitted ones  $I_t$  in Laue case[1] when X-ray energy is just below Ga K-edge (a) and 453.7eV below As K-edge (b). In (a), the rocking curves of  $I_h$  and  $I_t$  are anti-phase [2], while in (b), the maximum intensities due to anomalous transmission for  $I_h$  and  $I_t$  appear at the same angle and fringes in their tails are in-phase with each other. Figs. 2(a) and (b) shows

the topographs recorded at X-ray energies corresponding to those in Figs. 1(a) and (b), respectively. The interference fringes are clearly observed at the upper side of defect  $\alpha$  (see arrow in (a)). The area around the defect  $\alpha$  shows a dark band in (b).

Fig.3 shows a secondary electron image of the same region as in Fig.2 observed from the incident surface of X-ray by SEM (Scanning Electron Microscope). Along the defect band observed in the topographs in Fig. 2, many ditches are observed running in the [110] direction.

It is noted that topography making use of resonant scattering is very

useful not only to obtain information on the strain around a defect from the interference fringes in Fig. 2(a) but also to obtain the structural information of the defect from the image contrast caused by Borrmann effect in Fig. 2(b).

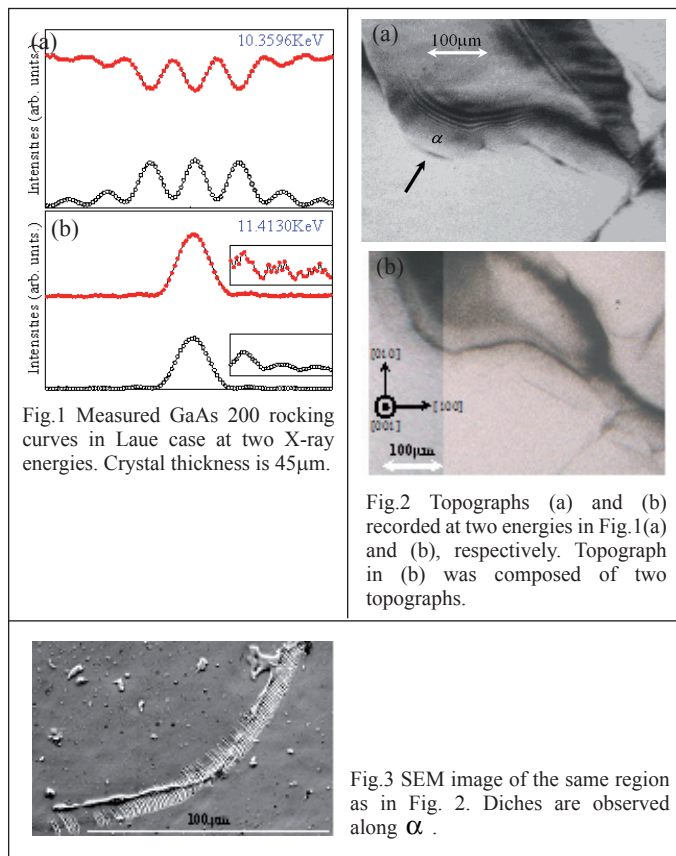


Fig.1 Measured GaAs 200 rocking curves in Laue case at two X-ray energies. Crystal thickness is 45 μm.

Fig.2 Topographs (a) and (b) recorded at two energies in Fig.1 (a) and (b), respectively. Topograph in (b) was composed of two topographs.

Fig.3 SEM image of the same region as in Fig. 2. Ditches are observed along  $\alpha$ .

[1] R. Negishi et al, T. Fukamachi, M. Yoshizawa, K. Hirano, Ki. Hirano, T. Kawamura, *J. Phys. Soc. Jpn.*, **2008**, *77*, 023709-1-3. [2] R. Negishi, T. Fukamachi, M. Yoshizawa, Ken. Hirano, Kei. Hirano, T. Kawamura, *Phys. Status Solidi A*, **2009**, *206*, 1865-1869.

**Keywords:** crystal structure factor, phase difference, GaAs

### MS33.P05

*Acta Cryst.* (2011) **A67**, C442

#### Conceptual design of the coherent X-ray scattering beamline at the taiwan photon source

Yu-Shan Huang,<sup>a</sup> Chi-Yi Huang,<sup>a</sup> Chien-Hung Chang,<sup>a</sup> Wen-Yan Peng,<sup>a</sup> U-Ser Jeng,<sup>a</sup> Chung-Yuan Mou,<sup>b</sup> Tsang-Lang Lin,<sup>c</sup> and Hsin-Lung Chen,<sup>c</sup> <sup>a</sup>National Synchrotron Radiation Research Center, Hsinchu 30076, (Taiwan). <sup>b</sup>National Taiwan University, Taipei 10617, (Taiwan). <sup>c</sup>National Tsing Hua University, Hsinchu 30013, (Taiwan). E-mail: jade@nsrrc.org.tw

The coherent X-ray scattering beamline is one of the first phase beamlines designed for the Taiwan Photon Source, a new 3 GeV ring under construction at the National Synchrotron Radiation Research Center in Taiwan. With an in-vacuum undulator, this beamline will provide highly coherent beam mainly for X-ray photon correlation spectroscopy as well as small angle X-ray scattering experiments. The beamline is designed to operate in the energy range 5-20 keV, suitable for most conventional SAXS, including anomalous measurements. A vertical focusing mirror collimates the beam to preserve the coherent photons with compatible coherent lengths in vertical and horizontal

directions. The horizontal coherence is nevertheless filtered by pairs of well polished slits for coherent experiments. An additional horizontal mirror focuses the incoherent beam horizontally for conventional SAXS experiments. The beamline can provide in either high flux mode or high energy resolution mode by changing monochromator's diffractive objects from silicon crystals to multilayers.

**Keywords:** beamline optical design, coherent scattering, small-angle x-ray scattering

### MS33.P06

*Acta Cryst.* (2011) **A67**, C442

#### Real-structure anisotropy in GaMnAs layers

Z. Šourek, M. Kopecký, J. Kub, J. Fábry, V. Novák, and M. Cukr, *Institute of Physics of AV CR, Na Slovance 2, 182 21 Prague (Czech Republic)*. E-mail: sourek@fzu.cz

The three-dimensional diffuse scattering pattern of a thick GaMnAs layer (layer thickness of 500 nm, Mn concentration of 7%) was measured in order to study the short range ordering of atoms in the layer. The layer was grown on a standard 2-inch GaAs wafer in our institute by means of the low-temperature molecular beam epitaxy. The experiment was carried on the diffraction beamline at the ELETTRA synchrotron radiation facility. The photon energy of 10 keV, i.e. slightly below the K absorption edge of Ga, was selected in order to avoid the fluorescence from the sample. The sample was mounted on the Kappa goniometer, a two-axis tilt stage was used in order to align the normal to the sample surface parallel to the phi-axis of the goniometer. This makes possible to scan a large volume of the reciprocal space by rotation the sample around its surface normal without changing the angle of incidence. The measurement was carried out in grazing incidence in order to hinder the penetration of the incident X-ray photons into the bulk - the beam was incident on the sample at a grazing angle of 0.3°. The scattered intensity in a large three-dimensional region of the reciprocal space of the GaMnAs layer was measured by recording a set of two-dimensional frames on a large CCD detector at different phi angles.

A three-dimensional map of intensities in the reciprocal space constructed from the set of two-dimensional CCD frames revealed thin one-dimensional features in the directions [111] and [-1-11]. Evidently, these features indicate the presence of stacking faults in crystallographic planes (111) and (-1-11). On the other hand, there were observed no stacking faults in the planes (-111) and (1-11). Structural models with intrinsic, extrinsic and twin stacking faults were created, including the combinations of individual types of stacking faults. The calculated X-ray scattering patterns from the model structures were compared to the experimental data. The same experiment was repeated using a thin GaMnAs layer (thickness 35 nm) and for the same samples after the annealing at the temperature of 200°C for the period of 10 hours. No appreciable difference in the scattering patterns of GaMnAs layers was observed. The relation of this structural anisotropy to the observed magnetic anisotropy is the subject of our further studies.

*This work was supported by the Grant Agency of the Academy of Sciences of the Czech Republic No. A 100100915 and the Institute of Physics' Institutional Research Plans Nos. Z10100520 and Z10100523.*

**Keywords:** X-ray diffuse scattering, magnetic semiconductors

### MS33.P07

*Acta Cryst.* (2011) **A67**, C442-C443

**Coherent bragg imaging of strained semi-conductor nano-**